

A Direct Determination of Molecular Structure: DL-*iso*Cryptopleurine Methiodide

By J. FRIDRICHSONS AND A. McL. MATHIESON

Chemical Physics Section, Division of Industrial Chemistry, Commonwealth Scientific and Industrial Research Organization, Melbourne, Australia

(Received 3 March 1955 and in revised form 8 July 1955)

DL-*iso*Cryptopleurine methiodide, a derivative of cryptopleurine, is monoclinic with unit cell dimensions, $a = 9.95$, $b = 24.2$, $c = 9.95$ Å, $\beta = 112^\circ$ and space group $P2_1/n$. Starting only with the empirical formula, $C_{25}H_{30}O_3NI$, and using no assumptions regarding the structure or normal bond lengths and angles, the crystal structure has been solved in a direct manner by the use of the 'heavy-atom' technique combined with a new application of generalized projections, the principle of which is as follows.

The data for each layer about one axis, e.g. Hkl , can be combined to yield a *modulus projection*,

$$|q_H(y, z)| = [C_H^2(y, z) + S_H^2(y, z)]^{\frac{1}{2}}.$$

This projection will in its main features be the same as $q_0(y, z)$, the *normal projection* derived from OkI data. Hence, from n layers, n views of the same projection can be obtained. For such 'heavy-atom' compounds, since signs initially can be fixed only by the 'heavy-atom' contribution, the projections both normal and modulus will be in error *but* errors in the n projections will not coincide since each projection is derived from a different set of data. Hence it is possible to combine several of the unrefined modulus projections with the unrefined normal projection to obtain the correct atom locations (y, z parameters). Then the approximate x parameters can be assessed from $C_1(y, z)$ and $S_1(y, z)$ and refinement carried through.

*iso*Cryptopleurine is shown to be 2':3':6'-trimethoxyphenanthro (9':10'-2:3) quinolizidine and this analysis constitutes the first observation of the phenanthreno (9':10'-2:3) quinolizidine ring system.

1. Introduction

In the structure analyses of moderately complex organic molecules (15–50 atoms excluding hydrogen) mainly by the use of 'heavy-atom' derivatives (for a review, see Mathieson, 1955), chemical evidence has been used implicitly or explicitly to guide (a) in the selection of probable molecular models and (b) in the allocation of the correct atom types to the peaks in the electron-density distribution. In the present paper we have attempted to demonstrate in a practical manner that the chemical information is not a necessary adjunct to the analysis (apart from a rough empirical formula) and that the X-ray method of determining the molecular structure of such compounds can be carried out solely on the basis of the diffraction data. For this purpose we required a compound about which chemical evidence of a structural nature was minimal. We are therefore grateful to Drs J. R. Price and E. Gellert, of the Organic Chemistry Section of this Division, for making available to us crystals of *isocryptopleurine* methiodide, a derivative of the alkaloid, cryptopleurine.

Neither the structure of cryptopleurine or of its derivatives was known, nor had any probable formulation been proposed (Gellert & Riggs, 1954). Chemical evidence of structural interest regarding *isocryptopleurine* methiodide was limited to (a) the empirical formula, (b) the presence of three methoxy groups

and (c) the similarity of the ultra-violet spectrum of cryptopleurine and its derivatives to that of phenanthrene and triphenylene. From the infra-red absorption spectra, no structural information was obtained. Because of the paucity of information, this compound therefore provided an excellent opportunity to illustrate that X-ray techniques can determine molecular structures in a direct manner.

A brief note of the result of this analysis has been published (Fridrichsons & Mathieson, 1954*a*) while a description of the method of analysis was presented at the Third International Congress on Crystallography (Fridrichsons & Mathieson, 1954*b*).

2. Experimental

The crystals were prepared by Dr E. Gellert by repeated slow crystallizations from methanol. They are tabular, with (010) the principal face, the edges of the plate being parallel to a and c . Measurement of rotation and equi-inclination Weissenberg photographs established the unit cell as monoclinic with

$$a = 9.95, b = 24.2, c = 9.95 \text{ \AA}; \beta = 112^\circ,$$

the space group being $P2_1/n$. The derivation of the space group revealed that the specimen was a racemate. With four units of $C_{25}H_{30}O_3NI$, the calculated density was 1.548 g.cm.^{-3} , that measured being 1.54 g.cm.^{-3} .

Intensity data for $hk0$, hkh , $0kl$, $1kl$ and $5kl$ spectra were collected on equi-inclination Weissenberg photographs. Two packs, each of four films (Ilford Industrial Type G), were exposed for 30 hr. and 1 hr., respectively. The intensities were estimated by comparison against a scale of standards. The dimensions of the crystal were $0.40 \times 0.18 \times 0.28$ mm. Intensities of $hk0$ and $0kl$ spectra were corrected for absorption, $\mu(\text{Cu } K\alpha) = 125 \text{ cm}^{-1}$, by a modification of the method of Joel, Vera & Garaycochea (1953). The absorption corrections were estimated for a variety of points in reciprocal space and the results were contoured; this enabled the corrections to be derived and applied more rapidly. The contour map of absorption corrections for $0kl$ spectra could be used also for $1kl$ spectra since the equi-inclination angle, μ_1 , for the first-layer data is small (4.4°) and the absorption corrections do not vary rapidly with μ_1 in this region. It was not considered that the use of the correction map could be extended to the $5kl$ data, and therefore no absorption corrections have been applied to these reflexions. The observed structure amplitudes were placed on an absolute basis at a later stage by comparison with the calculated values. The scaling and temperature factors were derived from plots of $\log \{ \sum |F_c| \div \sum |F_o| \}$ against $\sin^2 \theta$, summations being made over ranges of $\sin^2 \theta$, $0.0-0.1$, $0.1-0.2$, etc. Values of B for the respective sets of reflexions are given in Table 1.

Table 1. *The reflexions used in the various Fourier syntheses*

$n_{\text{obs.}}$ is the number of reflexions observed, $n_{\text{tot.}}$ the total theoretically observable; $R_{\text{obs.}}$ and $R_{\text{tot.}}$ are the corresponding reliability indices.

The total number of non-equivalent reflexions observed was 1072 (theoretical, 1550), the mean values of $R_{\text{obs.}}$ and $R_{\text{tot.}}$ being 0.156 and 0.162 respectively.

hkl	$n_{\text{obs.}}$	$n_{\text{tot.}}$	$R_{\text{obs.}}$	$R_{\text{tot.}}$	B (\AA^2)
$0kl$	215	290	0.135	0.145	3.9
$1kl$	389	570	0.177	0.187	3.9
$5kl$	341	490	0.154	0.158	4.8
$hk0$	182	280	0.129	0.129	5.3

Calculation of Fourier syntheses was carried out with 3° Beevers-Lipson strips (Beevers, 1952a), a and c being subdivided into 60 parts (0.166 \AA) and b into 120 parts (0.2017 \AA). The carbon and oxygen contributions to the structure amplitudes were calculated with 3° Beevers-Lipson strips, the interpolation method (Beevers, 1952b) being used. The scattering curve for I was taken from *Internationale Tabellen zur Bestimmung von Kristallstrukturen* (1935) while those for C, N and O were based on McWeeny's (1951) values.

During the progress of the analysis, the assessment of atom locations deduced from the various electron-density distributions was greatly facilitated by the use of a suitable method of display. On a thick cork mat was placed an ac cross-section of the unit cell subdivided into 60×60 sections. Each atom was represented by a wooden ball, supported on a brass rod whose length represented the y parameter. The rod was then inserted in the cork mat at the appropriate x, z position.

3. Structure analysis

The initial step was to locate the iodine atoms by computing Patterson functions, $P(y, z)$ and $P(x, y)$. The approximate parameters of the iodine atoms were refined by calculation of Fourier projections, ${}_1\rho_0(y, z)$ and ${}_1\rho_0(x, y)$ (Fig. 1(a) and (b)), those terms being used whose signs could be assumed as fixed by the iodine contribution, i.e. if the geometrical structure factor was > 0.1 (max. 1.0). On the basis of the two projections, an ambiguity in the values of the parameter existed. If x and y are defined, the third parameter may be z or $1-z$. This difficulty was resolved by consideration of a suitable third projection along the $[\bar{1}0\bar{1}]$ axis which lies at 124° to both the $[100]$ and $[001]$ axes. From inspection of the hkh structure amplitudes, the correct choice for the z parameter was made. A Fourier projection, ${}_1\rho_0(x-z, y)$ was then computed with the hkh spectra, the majority of the term-signs being fixed by the iodine contribution.

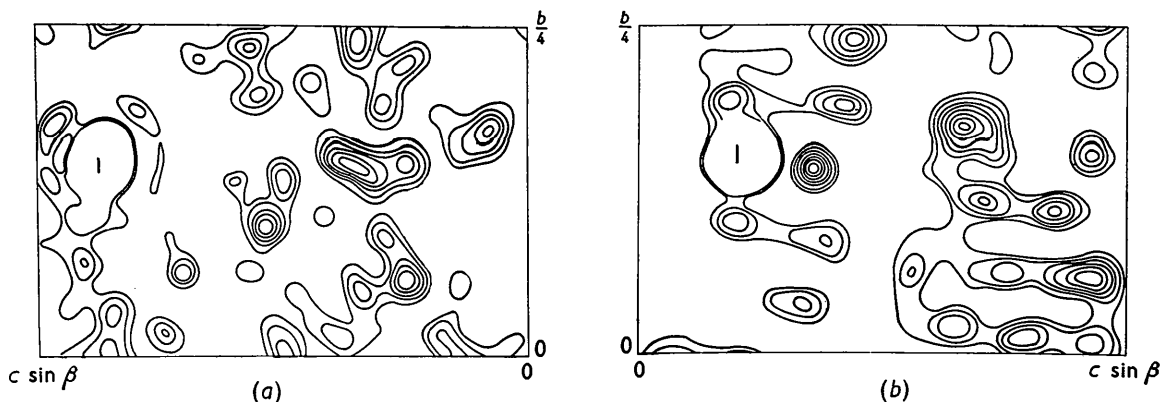


Fig. 1. (a) ${}_1\rho_0(y, z)$ and (b) ${}_1\rho_0(x, y)$ are the unrefined normal projections of electron density down the a and c axes respectively.

None of the contour maps, ${}_1\rho_0(x, y)$, ${}_1\rho_0(y, z)$ or ${}_1\rho_0(x-z, y)$ showed a distribution which might correspond to the molecule or any part thereof, e.g. the phenanthrene ring suggested by the ultraviolet spectrum. This was not to be expected since the projection axes are all of the order of 10 Å and there is latitude for extensive overlap of atoms. Since no chemical structure for this molecule had so far been proposed, it was not possible to proceed by the usual method of adjusting such a model over two projections until the approximately correct fit was achieved, and then refining. It was therefore clear that the structure of this molecule must be determined *solely* from the diffraction data. The problem was therefore restricted to that of locating 29 'light' atoms in the asymmetric volume of the unit cell. By the nature of the problem, nitrogen and oxygen atoms could not be differentiated from the carbon atoms and hence, for the initial stage of the investigation, all atoms were assumed to have the scattering power of carbon. Since there was no indication of the possible location of the molecules in the unit cell, attention was focused on a purely arbitrary but convenient asymmetric volume, V_a , enclosed by $x = 0$ to a , $y = 0$ to $\frac{1}{4}b$ and $z = 0$ to c . When the 29 atoms have been located in V_a , the particular grouping of atoms which constitute a molecule can be determined and then the distribution of molecules in the unit cell made evident.

The first attempt at a solution of the crystal structure was based on the use of the three unrefined projections, ${}_1\rho_0(x, y)$, ${}_1\rho_0(y, z)$ and ${}_1\rho_0(x-z, y)$. It was considered that, if these projections approximated sufficiently to the true electron-density distributions, it should be possible to extract from them the distribution of atoms in V_a . The first method tried was based on the following idea. For any given value of y , a minimum function (Buerger, 1951),

$$M_y(x, z) = M[{}_1\rho_0(x, y), {}_1\rho_0(y, z), {}_1\rho_0(x-z, y)]$$

was extracted from the corresponding lines of the same y parameter in the three electron-density maps and the result contoured in the x, z plane. This was tested for several values of y , but did not lead to any resolution of atoms. The second method was based on an attempted correlation of the x, z and $x-z$ parameters of peaks at approximately the same y level, by visual inspection of the three contoured maps. Both methods failed and it was concluded that the three projections contained too many false features: (a) there were incompletely developed peaks where atoms did exist; (b) there were spurious peaks where no atoms occurred; and (c) such peaks as were correct were sufficiently in error in location to prevent correlation of the three projections.*

* The addition to the calculated structure amplitudes of contributions corresponding to the sampling of the unrefined Fourier maps at regions above a certain value of electron density (in a manner similar to that suggested by Carlisle & King (1954)) did not lead to further solution of the problem

An investigation in three dimensions was therefore necessary. However, the available computing facilities were insufficient for a complete three-dimensional study on such a large molecule and it was decided to test the applicability of generalized projections (Cochran & Dyer, 1952) in solving structures *ab initio*. Since the projection down the a axis, Fig. 1(a), appeared to offer the best resolution of atoms, the corresponding first-layer spectra, $1kl$, were used. The iodine contributions were calculated, and where the geometrical structure factor was > 0.1 (max. 1.0), the iodine sign was used for the corresponding observed structure amplitude. The components, ${}_1C_1$ and ${}_1S_1$, of the generalized projection, ${}_1\rho_1 = {}_1C_1 + i{}_1S_1$, were computed from (1) and (2):†

$$\left. \begin{aligned} C_1 &= \frac{2}{A} \sum_0^k \sum_0^l \left\{ F(1kl) + F(1k\bar{l}) \right\} \cos 2\pi ky \cos 2\pi lz \\ &\quad (h+k+l = 2n) \\ &\quad - \frac{2}{A} \sum_0^k \sum_0^l \left\{ F(1kl) - F(1k\bar{l}) \right\} \sin 2\pi ky \sin 2\pi lz \\ &\quad (h+k+l = 2n+1) \end{aligned} \right\} (1)$$

$$\left. \begin{aligned} S_1 &= -\frac{2}{A} \sum_0^k \sum_0^l \left\{ F(1kl) - F(1k\bar{l}) \right\} \cos 2\pi ky \sin 2\pi lz \\ &\quad (h+k+l = 2n) \\ &\quad - \frac{2}{A} \sum_0^k \sum_0^l \left\{ F(1kl) + F(1k\bar{l}) \right\} \sin 2\pi ky \cos 2\pi lz \\ &\quad (h+k+l = 2n+1) \end{aligned} \right\} (2)$$



Fig. 2. $|{}_1\rho_1(y, z)| = [{}_1C_1^2(y, z) + {}_1S_1^2(y, z)]^{1/2}$ is the first modulus projection using $1kl$ spectra.

The resultant distributions (not shown) contain a great deal of spurious detail. Since the atom locations are not known, even so far as their y, z parameters, one cannot use the component maps, ${}_1C_1$ and ${}_1S_1$, to extract x parameters. However, it was noted that

since the peaks corresponding to atoms are not known. That this method should fail is indicated by comparison of Fig. 1(a) and (b) with the corresponding final refined projections. It appeared that this type of 'refinement' tends merely to reproduce what one has inserted in the data.

† When referring to ${}_n\rho_r$, ${}_nC_r$ and ${}_nS_r$, the prefix n denotes the n th stage of refinement and the suffix r the particular layer.

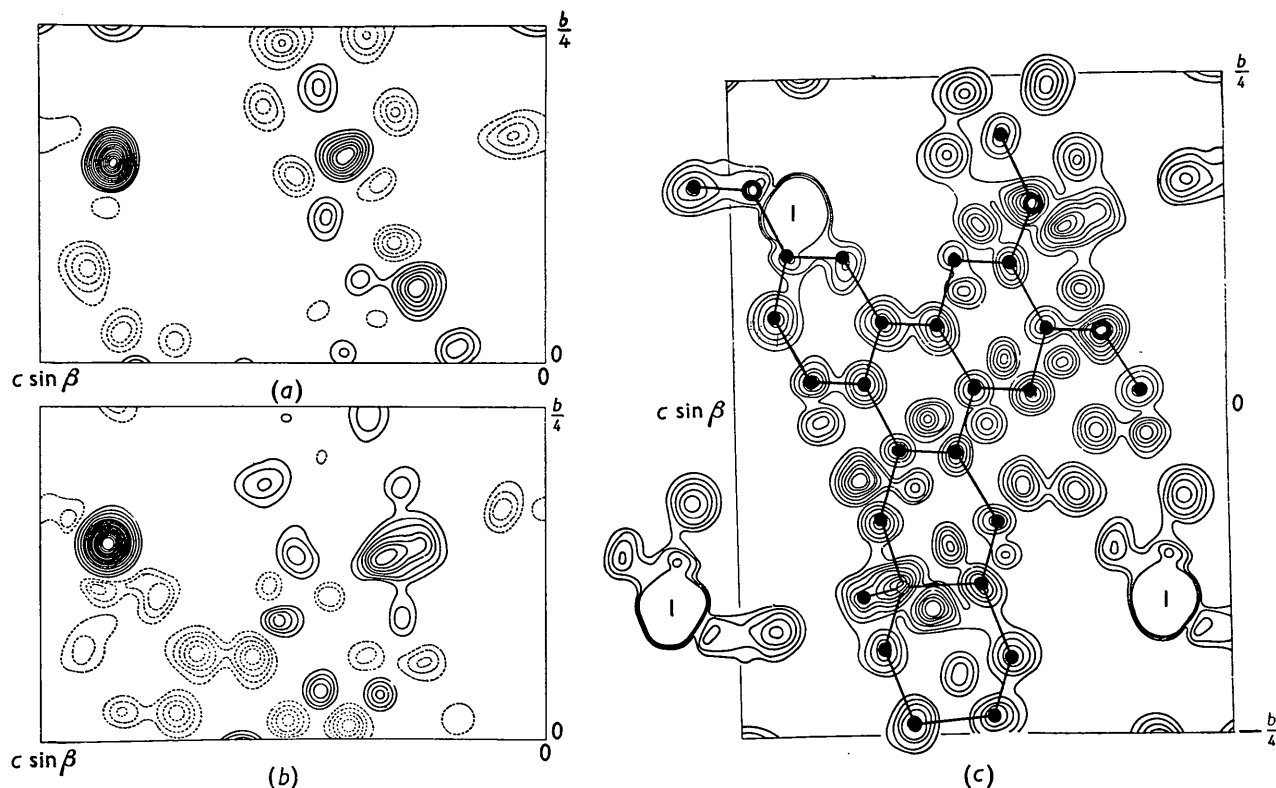


Fig. 3. (a) ${}_3C_1(y, z)$, (b) ${}_3S_1(y, z)$ and (c) $|{}_3\rho_1(y, z)|$. Contour levels are at intervals of $1 \text{ e.}\text{\AA}^{-2}$, beginning at $2 \text{ e.}\text{\AA}^{-2}$, except for iodine in ${}_3S_1$, where intervals are at $5 \text{ e.}\text{\AA}^{-2}$, beginning at $10 \text{ e.}\text{\AA}^{-2}$. Broken lines represent negative values of functions ${}_3C_1$ and ${}_3S_1$. The contours corresponding to iodine have been omitted from $|{}_3\rho_1|$ and in most of the subsequent figures. A diagram of one molecule is superimposed.

C_1 and S_1 could be combined to yield the *modulus* of the generalized projection, $|\rho_1| = [C_1^2 + S_1^2]^{1/2}$.*

The distribution $|\rho_1|$ is in essentials similar to ρ_0 , i.e. it represents the view of the unit-cell contents projected down the a axis and contains only y, z parameters, but is derived from data different from those used in the normal projection. The modulus projection $|{}_1\rho_1|$, Fig. 2, contained a great deal of spurious detail, as did ${}_1\rho_0$, Fig. 1(a), but as the two projections are based on non-equivalent sets of data, peaks corresponding to real atoms tend to coincide in location in the two maps while spurious peaks do not. It was therefore possible to derive from ${}_1\rho_0$ and $|{}_1\rho_1|$ an electron-density distribution which is more correct than either. To extract this information, the concept of a minimum function (Buerger, 1951) was again used and $M({}_1\rho_0, |{}_1\rho_1|)$ was contoured.† This distribution still contained spurious detail but 25 peaks were selected as authentic atom sites. The minimum function yielded the y, z parameters, and inspection of

* Only later was it noted that Clews & Cochran (1949) had computed this function, which they referred to as $R(h, y, z)$. They did not use this function to solve the structure, but to refine the parameters.

† When the solution was achieved, it was realized that the simpler summation function $\Sigma({}_1\rho_0, |{}_1\rho_1|)$ may have certain advantages for this purpose.

${}_1C_1$ and ${}_1S_1$ gave the approximate x parameters. Structure amplitudes, $1kl$, were then computed with the iodine atom and the 25 'light' atoms, the reliability index ($R = \Sigma||F_o| - |F_c|| / \Sigma|F_o|$) being reduced from 0.36 (with iodine only) to 0.23. The signs of about 40 terms, previously unused, were fixed and ${}_2C_1$ and ${}_2S_1$ were computed. The components were then combined to yield the modulus projection, $|{}_2\rho_1|$, which was a great improvement in appearance over $|{}_1\rho_1|$. Apart from the iodine peak, the distribution could be accounted for by 29 'light' atoms, 26 clearly resolved, and, of the three remaining, one was adjacent to and partially masked by the iodine atom and the two others too close together to permit clear resolution, but obviously corresponding to two atoms. There were no dubious features, all spurious peaks having been removed. The x parameter of each atom was determined by the relation, $2\pi x/a = \tan^{-1}({}_2S_1(y, z) / {}_2C_1(y, z))$, y, z being the parameters determined from $|{}_2\rho_1|$. As the location of each peak was transferred to the display-grid, it was possible to see two structural units taking shape in V_a . Each unit suggested a rational arrangement of atoms and, by transferring one unit across a centre of symmetry so as to link with the other unit, the whole molecule became clearly defined. No gross discrepancies in interatomic distances or

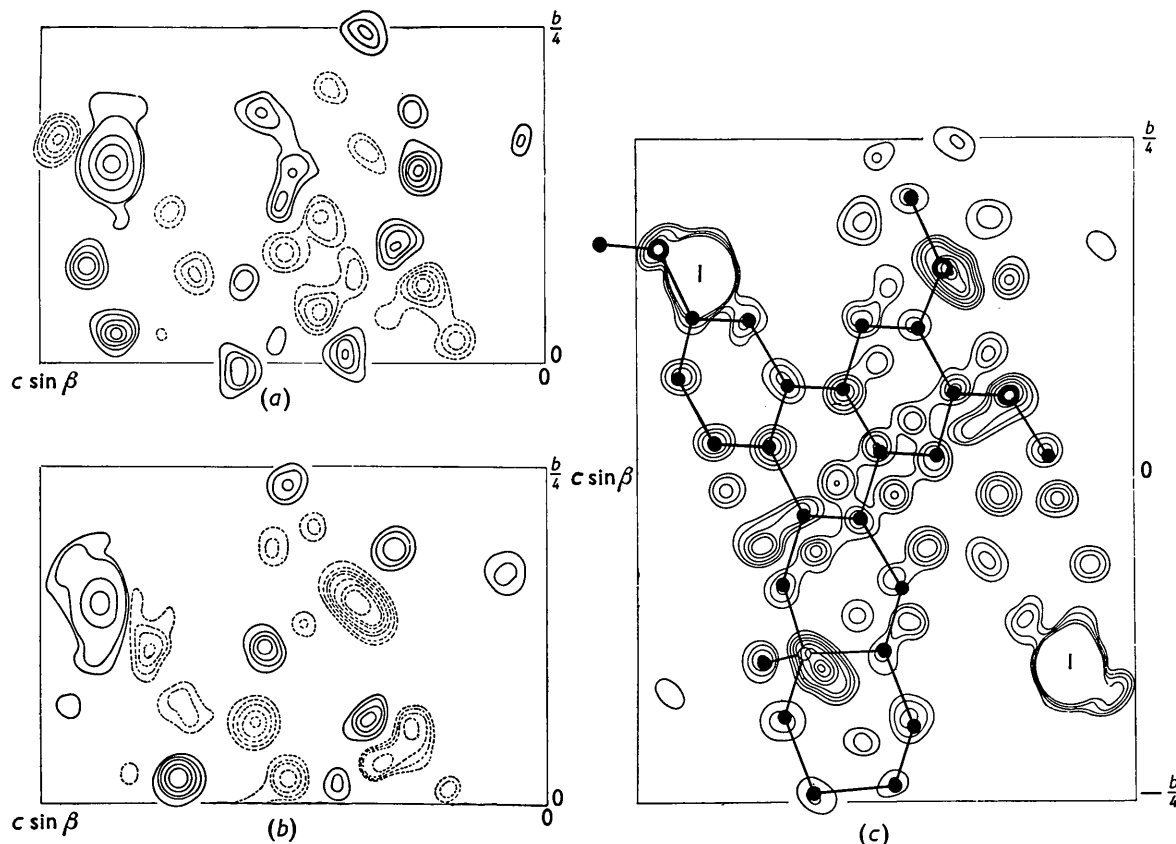


Fig. 4. (a) ${}_2C_5(y, z)$, (b) ${}_2S_5(y, z)$ and (c) ${}_2Q_5(y, z)$. Contour levels are at intervals of $0.5 \text{ e.}\text{\AA}^{-2}$, beginning at $1.5 \text{ e.}\text{\AA}^{-2}$, except in the case of the iodine atom, where higher contours are at intervals of $10 \text{ e.}\text{\AA}^{-2}$. The scale is absolute, as in Fig. 3: hence the lower atom peak heights.

angles occurred and the distribution of intermolecular approach distances afforded evidence of compact molecular packing in the crystal. At this stage, the structures of the crystal and the molecular skeleton had been solved in essentials and the later stages of the analysis were aimed at refinement of the atomic parameters and definition of atom types.

Although the majority of atom sites were unchanged, several transfers to different regions of V_a had occurred in ${}_2Q_1$ compared with ${}_1Q_1$ and also all 29 atoms had been located. Recalculation of the structure amplitudes, $1kl$, with the new and complete set of atomic coordinates reduced the reliability index to 0.19, and the signs of all observed terms could be fixed. ${}_3C_1$ and ${}_3S_1$ (Fig. 3(a) and (b)) were then computed, the 'less than' Fourier terms being included with either their calculated or limiting values. The corresponding modulus projection, ${}_3Q_1$ (Fig. 3(c)), showed excellent resolution of atoms and clearly indicated the heavier oxygen atoms (except one adjacent to the iodine atom). Even the nitrogen atom peak could be distinguished from the oxygen and carbon peaks. From ${}_3C_1$ and ${}_3S_1$, x parameters of all atoms were derived and the structure amplitudes for $5kl$ spectra were calculated. With the signs of the majority of terms thus

fixed, ${}_1C_5$ and ${}_1S_5$ were computed and combined to give the modulus projection ${}_1Q_5$ which showed good agreement with ${}_3Q_1$. Further refinement of x parameters was derived from the relation $2\pi.5x/a = \tan^{-1}{}_1S_5(y, z)/{}_1C_5(y, z)$, and these values were then the basis for recalculation of the $5kl$ structure amplitudes. ${}_2C_5$ and ${}_2S_5$ (Fig. 4(a) and (b)) were computed and combined to give the modulus projection ${}_2Q_5$ (Fig. 4(c)). $0kl$ structure amplitudes were calculated and the normal projection ${}_2Q_0(y, z)$ (Fig. 5(a); cf. Fig. 1(a)) was computed. To obtain the best y, z parameters, the three final a -axis projections were combined to give $Q_{\Sigma} = \frac{1}{2} \cdot {}_2Q_0 + {}_3Q_1 + {}_2Q_5$ (Fig. 5(b)). For confirmation of the x parameters, the $hk0$ structure amplitudes were computed ($R = 0.13$) and the projection down the c axis was computed, ${}_2Q_0(x, y)$ (Fig. 5(c); cf. Fig. 1(b)). The best x parameters were derived from a comparison of ${}_2C_5$, ${}_2S_5$ and ${}_2Q_0(x, y)$. The atomic parameters of the atoms of the asymmetric unit are given in Table 2, and the intramolecular distances and angles calculated from these parameters in Table 3 and Fig. 6(a). Some of the more important intermolecular approach distances are also listed in Table 3 and Fig. 6(b). The observed and the calculated structure amplitudes are compared in Table 4.

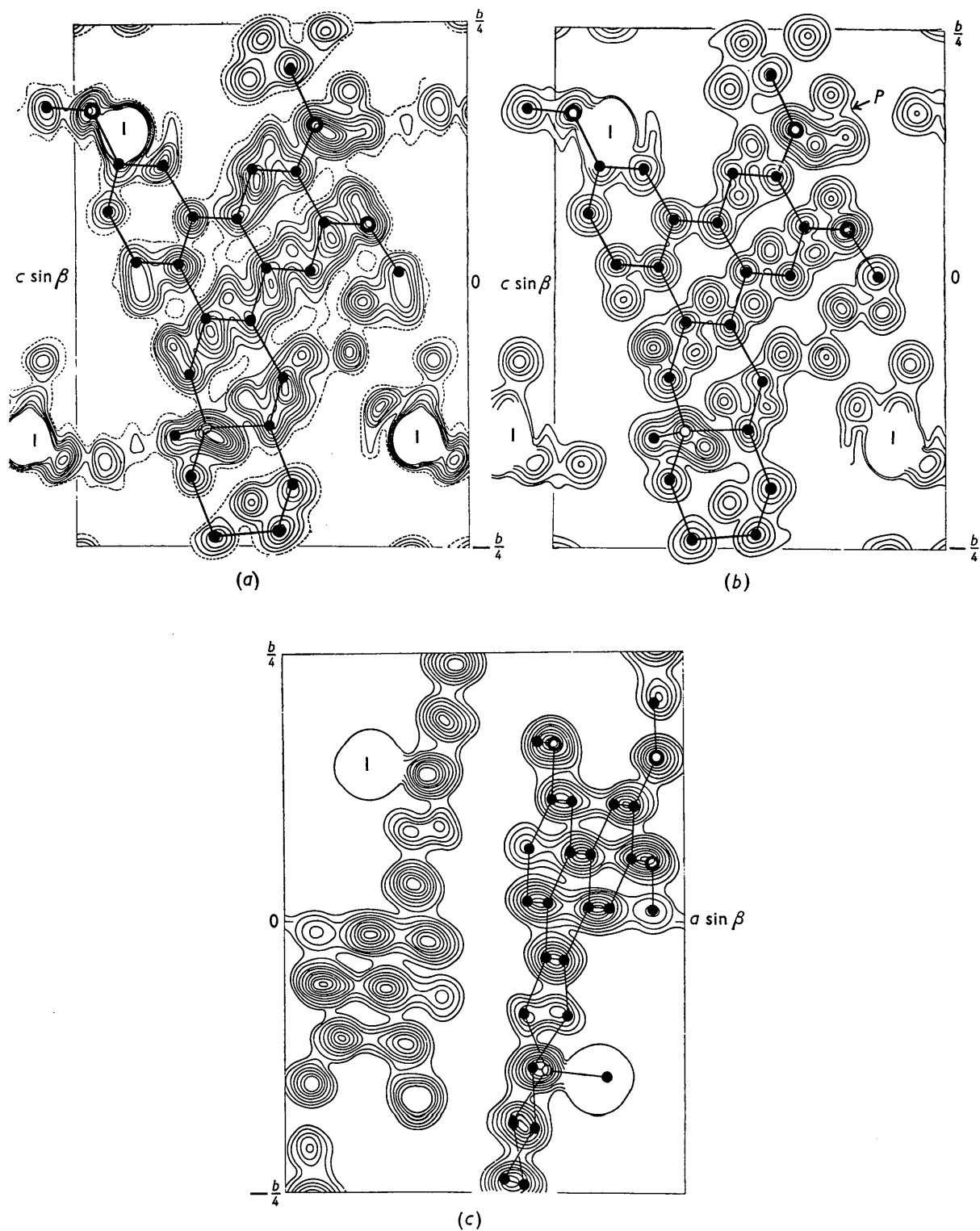


Fig. 5. (a) $\rho_0(y, z)$ is the normal projection down the a axis derived from $0kl$ spectra. Contour levels are at intervals of $1 \text{ e.}\text{\AA}^{-2}$, beginning at $3 \text{ e.}\text{\AA}^{-2}$ (broken line). (b) $\rho_x(y, z) = \frac{1}{2}\rho_0(y, z) + |\rho_1(y, z)| + |\rho_5(y, z)|$ is the distribution obtained by combining the projections derived from $0kl$, $1kl$ and $5kl$ spectra. In region P , carbon, nitrogen and oxygen atoms are adjacent and can be differentiated on the basis of peak height. (c) $\rho_0(x, y)$ is the normal projection down the c axis derived from $hk0$ spectra. Contour levels are at intervals of $1 \text{ e.}\text{\AA}^{-2}$, beginning at $4 \text{ e.}\text{\AA}^{-2}$.

Table 2. Atomic parameters of one asymmetric unit (molecule)

Atom	x/a	y/b	z/c
I	0.778	-0.148	1.135
O ₍₁₎	0.922	0.0567	0.250
O ₍₂₎	0.933	0.153	0.383
O ₍₃₎	0.682	0.167	0.955
N	0.657	-0.139	0.667
C ₍₁₎	0.817	0.0117	0.398
C ₍₂₎	0.873	0.0583	0.360
C ₍₃₎	0.880	0.108	0.433
C ₍₄₎	0.833	0.110	0.547
C ₍₅₎	0.722	0.113	0.775
C ₍₆₎	0.672	0.116	0.888
C ₍₇₎	0.608	0.0692	0.917
C ₍₈₎	0.610	0.0208	0.845
C ₍₉₎	0.658	-0.0333	0.667
C ₍₁₀₎	0.703	-0.0363	0.552
C ₍₁₁₎	0.767	0.0138	0.512
C ₍₁₂₎	0.775	0.0625	0.585
C ₍₁₃₎	0.722	0.0650	0.698
C ₍₁₄₎	0.668	0.0188	0.737
C ₍₁₅₎	0.712	-0.0892	0.468
C ₍₁₆₎	0.623	-0.136	0.505
C ₍₁₇₎	0.630	-0.193	0.445
C ₍₁₈₎	0.547	-0.238	0.483
C ₍₁₉₎	0.600	-0.242	0.648
C ₍₂₀₎	0.575	-0.186	0.705
C ₍₂₁₎	0.600	-0.0858	0.708
C ₍₂₂₎	0.808	-0.146	0.747
C ₍₂₃₎	0.923	0.0108	0.172
C ₍₂₄₎	0.937	0.206	0.448
C ₍₂₅₎	0.637	0.169	1.072

4. Structure and configuration of the molecule

The structure analysis revealed that the molecule consists of five six-membered rings fused together, with one monatomic and three diatomic substituents (ignoring hydrogen). From the peak heights in the electron-density distribution, the nitrogen and three oxygen atoms can be differentiated from the carbon atoms, showing that nitrogen is common to rings *A* and *B* (Fig. 6(a)) and has C₍₂₂₎ attached to it, while O₍₁₎-C₍₂₃₎, O₍₂₎-C₍₂₄₎ and O₍₃₎-C₍₂₅₎ constitute the diatomic substituent groups. The bond lengths and angles (Table 3) within the *CDE* ring system indicate an aromatic nucleus (phenanthrene) and this is confirmed by the fact that the mean deviation of atoms C₍₁₎ . . . C₍₁₄₎ from the plane *L*,

$$0.9106x' - 0.2360y + 0.3391z' - 7.1211 = 0$$

is 0.02 Å (maximum deviation, 0.08 Å).^{*} Furthermore, as is to be expected, C₍₁₅₎, C₍₂₁₎, O₍₁₎, O₍₂₎ and O₍₃₎ lie in this plane with a mean deviation of 0.04 Å (max. 0.06 Å). The interatomic distances of atoms attached to O₍₁₎, O₍₂₎ and O₍₃₎ are in agreement with single-bond values and hence the groups, O₍₁₎-C₍₂₃₎, O₍₂₎-C₍₂₄₎ and O₍₃₎-C₍₂₅₎ are methoxyl groups in substituent positions 2, 3 and 6 of the phenanthrene

^{*} The coordinates x' , z' refer to rectilinear axes, a' normal to c and c' collinear with c . Hence $x' = x \sin \beta$ and $z' = z + x \cos \beta$.

Table 3. Bond lengths and angles, and approach distances

(a) Intramolecular bond lengths					
Bond	Length (Å)	Bond	Length (Å)	Bond	Length (Å)
O ₍₁₎ -C ₍₂₎	1.35	C ₍₁₃₎ -C ₍₅₎	1.39	C ₍₁₀₎ -C ₍₁₅₎	1.54
O ₍₁₎ -C ₍₂₃₎	1.35	C ₍₅₎ -C ₍₆₎	1.40	C ₍₁₅₎ -C ₍₁₆₎	1.55
O ₍₂₎ -C ₍₃₎	1.36	C ₍₆₎ -C ₍₇₎	1.37	C ₍₁₆₎ -C ₍₁₇₎	1.52
O ₍₂₎ -C ₍₂₄₎	1.42	C ₍₇₎ -C ₍₈₎	1.37	C ₍₁₇₎ -C ₍₁₈₎	1.52
O ₍₃₎ -C ₍₆₎	1.38	C ₍₈₎ -C ₍₁₄₎	1.40	C ₍₁₈₎ -C ₍₁₉₎	1.52
O ₍₃₎ -C ₍₂₅₎	1.40	C ₍₁₄₎ -C ₍₁₃₎	1.36	C ₍₁₉₎ -C ₍₂₀₎	1.54
C ₍₁₎ -C ₍₂₎	1.37	C ₍₁₁₎ -C ₍₁₂₎	1.37	C ₍₂₀₎ -N	1.53
C ₍₂₎ -C ₍₃₎	1.40	C ₍₁₎ -C ₍₁₁₎	1.39	N-C ₍₁₆₎	1.53
C ₍₃₎ -C ₍₄₎	1.38	C ₍₉₎ -C ₍₁₀₎	1.38	N-C ₍₂₂₎	1.42
C ₍₄₎ -C ₍₁₂₎	1.39	C ₍₉₎ -C ₍₁₄₎	1.43	N-C ₍₂₁₎	1.51
C ₍₁₂₎ -C ₍₁₃₎	1.42	C ₍₁₀₎ -C ₍₁₁₎	1.47	C ₍₂₁₎ -C ₍₉₎	1.52

(b) Intramolecular bond angles			
Bonds	Angle (°)	Bonds	Angle (°)
C ₍₂₎ -O ₍₁₎ -C ₍₂₃₎	124	C ₍₁₁₎ -C ₍₁₂₎ -C ₍₁₃₎	119
C ₍₃₎ -O ₍₂₎ -C ₍₂₄₎	119	C ₍₁₂₎ -C ₍₁₃₎ -C ₍₅₎	123
C ₍₆₎ -O ₍₃₎ -C ₍₂₅₎	115	C ₍₁₂₎ -C ₍₁₃₎ -C ₍₁₄₎	120
C ₍₁₁₎ -C ₍₁₎ -C ₍₂₎	120	C ₍₅₎ -C ₍₁₃₎ -C ₍₁₄₎	117
C ₍₁₎ -C ₍₂₎ -O ₍₁₎	120	C ₍₁₃₎ -C ₍₅₎ -C ₍₆₎	123
C ₍₁₎ -C ₍₂₎ -C ₍₃₎	121	C ₍₅₎ -C ₍₆₎ -C ₍₇₎	117
C ₍₃₎ -C ₍₂₎ -O ₍₁₎	119	C ₍₅₎ -C ₍₆₎ -O ₍₃₎	116
C ₍₂₎ -C ₍₃₎ -C ₍₄₎	119	C ₍₇₎ -C ₍₆₎ -O ₍₃₎	125
C ₍₂₎ -C ₍₃₎ -O ₍₂₎	116	C ₍₆₎ -C ₍₇₎ -C ₍₈₎	120
C ₍₄₎ -C ₍₃₎ -O ₍₂₎	125	C ₍₇₎ -C ₍₈₎ -C ₍₁₄₎	121
C ₍₃₎ -C ₍₄₎ -C ₍₁₂₎	120	C ₍₈₎ -C ₍₁₄₎ -C ₍₁₃₎	120
C ₍₄₎ -C ₍₁₂₎ -C ₍₁₁₎	121	C ₍₈₎ -C ₍₁₄₎ -C ₍₉₎	119
C ₍₄₎ -C ₍₁₂₎ -C ₍₁₃₎	120	C ₍₉₎ -C ₍₁₄₎ -C ₍₁₃₎	122
C ₍₁₄₎ -C ₍₉₎ -C ₍₁₀₎	120	N-C ₍₁₆₎ -C ₍₁₇₎	117
C ₍₁₄₎ -C ₍₉₎ -C ₍₂₁₎	120	C ₍₁₆₎ -C ₍₁₇₎ -C ₍₁₃₎	116
C ₍₁₀₎ -C ₍₉₎ -C ₍₂₁₎	118	C ₍₁₇₎ -C ₍₁₈₎ -C ₍₁₉₎	109
C ₍₉₎ -C ₍₁₀₎ -C ₍₁₁₎	120	C ₍₁₈₎ -C ₍₁₉₎ -C ₍₂₀₎	107
C ₍₁₀₎ -C ₍₁₁₎ -C ₍₁₂₎	120	C ₍₁₉₎ -C ₍₂₀₎ -N	114
C ₍₁₀₎ -C ₍₁₁₎ -C ₍₁₎	121	C ₍₂₀₎ -N-C ₍₁₆₎	113
C ₍₁₎ -C ₍₁₁₎ -C ₍₁₂₎	119	C ₍₁₆₎ -N-C ₍₂₁₎	106
C ₍₁₁₎ -C ₍₁₀₎ -C ₍₁₅₎	115	C ₍₂₀₎ -N-C ₍₂₂₎	110
C ₍₉₎ -C ₍₁₀₎ -C ₍₁₅₎	125	C ₍₂₁₎ -N-C ₍₂₂₎	110
C ₍₁₀₎ -C ₍₁₅₎ -C ₍₁₆₎	110	C ₍₁₆₎ -N-C ₍₂₂₎	111
C ₍₁₅₎ -C ₍₁₆₎ -N	112	C ₍₂₀₎ -N-C ₍₂₁₎	105
C ₍₁₅₎ -C ₍₁₆₎ -C ₍₁₇₎	118	N-C ₍₂₁₎ -C ₍₉₎	115

(c) Nearest approach distances			
Atoms	d (Å)	Atoms	d (Å)
I-C ₍₂₅₎	3.96	I-C ₍₂₅₎	3.90
I-O ₍₂₎	4.56	O ₍₃₎ -C ₍₁₇₎	4.08
I-C ₍₁₇₎	4.03	C ₍₁₈₎ -C ₍₂₄₎	4.36
I-C ₍₁₉₎	4.10	C ₍₅₎ -C ₍₁₆₎	3.56
I-C ₍₂₄₎	4.06	C ₍₅₎ -C ₍₂₁₎	4.72
I-C ₍₁₈₎	4.44	C ₍₄₎ -C ₍₂₁₎	4.14
I-O ₍₃₎	4.35	C ₍₃₎ -C ₍₂₁₎	4.45
O ₍₃₎ -C ₍₁₉₎	3.50	C ₍₁₄₎ -C ₍₁₀₎	3.76
O ₍₃₎ -C ₍₂₄₎	3.93	O ₍₂₎ -C ₍₂₂₎	3.30
O ₍₃₎ -C ₍₁₈₎	3.44		

nucleus. The atoms C₍₉₎ and C₍₁₀₎ of the phenanthrene ring system form part of the adjacent ring *B*. Apart from C₍₉₎-C₍₁₀₎, the bond lengths within the *AB* ring system are normal single-bond C-C or C-N values. The angular nitrogen atom common to rings *A* and *B* is quaternary. The configuration of the *AB* (quinolizidine) ring system is partly determined by the associated phenanthrene nucleus. Thus the bonds C₍₁₀₎-C₍₁₅₎ and C₍₉₎-C₍₂₁₎ are maintained in the plane

Table 4. Comparison of observed and calculated structure amplitudes

k	P _c	F _o	k	P _c	F _o	k	P _c	F _o	k	P _c	F _o	k	P _c	F _o	k	P _c	F _o	k	P _c	F _o	k	P _c	F _o	k	P _c	F _o	k	P _c	F _o																																																																																																																																																																																																																																																																																																																																																																																																																																																																																																																																																																																																																																																																																																																																																																																																																																																																																																																																																																																																																																																																																																																																																																																																																																																																																																																																																																																																																																																																																						
2	+70	62	1	-109	110	0	+49	59	0	+36	33	17	+37	38	0	+37	43	0	-218	161	20	+2	<9	8	-6	<9	1	+23	<9	9	-5	<9	2	+25	<9	10	+9	<9	3	+31	<9	11	+10	<9	4	+37	<9	12	+11	<9	5	+43	<9	13	+12	<9	6	+49	<9	14	+13	<9	7	+55	<9	15	+14	<9	8	+61	<9	16	+15	<9	9	+67	<9	17	+16	<9	10	+73	<9	18	+17	<9	11	+79	<9	19	+18	<9	12	+85	<9	20	+19	<9	13	+91	<9	21	+20	<9	14	+97	<9	22	+21	<9	15	+103	<9	23	+22	<9	16	+109	<9	24	+23	<9	17	+115	<9	25	+24	<9	18	+121	<9	26	+25	<9	19	+127	<9	27	+26	<9	20	+133	<9	28	+27	<9	21	+139	<9	29	+28	<9	22	+145	<9	30	+29	<9	23	+151	<9	31	+30	<9	24	+157	<9	32	+31	<9	25	+163	<9	33	+32	<9	26	+169	<9	34	+33	<9	27	+175	<9	35	+34	<9	28	+181	<9	36	+35	<9	29	+187	<9	37	+36	<9	30	+193	<9	38	+37	<9	31	+199	<9	39	+38	<9	32	+205	<9	40	+39	<9	33	+211	<9	41	+40	<9	34	+217	<9	42	+41	<9	35	+223	<9	43	+42	<9	36	+229	<9	44	+43	<9	37	+235	<9	45	+44	<9	38	+241	<9	46	+45	<9	39	+247	<9	47	+46	<9	40	+253	<9	48	+47	<9	41	+259	<9	49	+48	<9	42	+265	<9	50	+49	<9	43	+271	<9	51	+50	<9	44	+277	<9	52	+51	<9	45	+283	<9	53	+52	<9	46	+289	<9	54	+53	<9	47	+295	<9	55	+54	<9	48	+301	<9	56	+55	<9	49	+307	<9	57	+56	<9	50	+313	<9	58	+57	<9	51	+319	<9	59	+58	<9	52	+325	<9	60	+59	<9	53	+331	<9	61	+60	<9	54	+337	<9	62	+61	<9	55	+343	<9	63	+62	<9	56	+349	<9	64	+63	<9	57	+355	<9	65	+64	<9	58	+361	<9	66	+65	<9	59	+367	<9	67	+66	<9	60	+373	<9	68	+67	<9	61	+379	<9	69	+68	<9	62	+385	<9	70	+69	<9	63	+391	<9	71	+70	<9	64	+397	<9	72	+71	<9	65	+403	<9	73	+72	<9	66	+409	<9	74	+73	<9	67	+415	<9	75	+74	<9	68	+421	<9	76	+75	<9	69	+427	<9	77	+76	<9	70	+433	<9	78	+77	<9	71	+439	<9	79	+78	<9	72	+445	<9	80	+79	<9	73	+451	<9	81	+80	<9	74	+457	<9	82	+81	<9	75	+463	<9	83	+82	<9	76	+469	<9	84	+83	<9	77	+475	<9	85	+84	<9	78	+481	<9	86	+85	<9	79	+487	<9	87	+86	<9	80	+493	<9	88	+87	<9	81	+499	<9	89	+88	<9	82	+505	<9	90	+89	<9	83	+511	<9	91	+90	<9	84	+517	<9	92	+91	<9	85	+523	<9	93	+92	<9	86	+529	<9	94	+93	<9	87	+535	<9	95	+94	<9	88	+541	<9	96	+95	<9	89	+547	<9	97	+96	<9	90	+553	<9	98	+97	<9	91	+559	<9	99	+98	<9	92	+565	<9	100	+99	<9	93	+571	<9	101	+100	<9	94	+577	<9	102	+101	<9	95	+583	<9	103	+102	<9	96	+589	<9	104	+103	<9	97	+595	<9	105	+104	<9	98	+601	<9	106	+105	<9	99	+607	<9	107	+106	<9	100	+613	<9	108	+107	<9	101	+619	<9	109	+108	<9	102	+625	<9	110	+109	<9	103	+631	<9	111	+110	<9	104	+637	<9	112	+111	<9	105	+643	<9	113	+112	<9	106	+649	<9	114	+113	<9	107	+655	<9	115	+114	<9	108	+661	<9	116	+115	<9	109	+667	<9	117	+116	<9	110	+673	<9	118	+117	<9	111	+679	<9	119	+118	<9	112	+685	<9	120	+119	<9	113	+691	<9	121	+120	<9	114	+697	<9	122	+121	<9	115	+703	<9	123	+122	<9	116	+709	<9	124	+123	<9	117	+715	<9	125	+124	<9	118	+721	<9	126	+125	<9	119	+727	<9	127	+126	<9	120	+733	<9	128	+127	<9	121	+739	<9	129	+128	<9	122	+745	<9	130	+129	<9	123	+751	<9	131	+130	<9	124	+757	<9	132	+131	<9	125	+763	<9	133	+132	<9	126	+769	<9	134	+133	<9	127	+775	<9	135	+134	<9	128	+781	<9	136	+135	<9	129	+787	<9	137	+136	<9	130	+793	<9	138	+137	<9	131	+799	<9	139	+138	<9	132	+805	<9	140	+139	<9	133	+811	<9	141	+140	<9	134	+817	<9	142	+141	<9	135	+823	<9	143	+142	<9	136	+829	<9	144	+143	<9	137	+835	<9	145	+144	<9	138	+841	<9	146	+145	<9	139	+847	<9	147	+146	<9	140	+853	<9	148	+147	<9	141	+859	<9	149	+148	<9	142	+865	<9	150	+149	<9	143	+871	<9	151	+150	<9	144	+877	<9	152	+151	<9	145	+883	<9	153	+152	<9	146	+889	<9	154	+153	<9	147	+895	<9	155	+154	<9	148	+901	<9	156	+155	<9	149	+907	<9	157	+156	<9	150	+913	<9	158	+157	<9	151	+919	<9	159	+158	<9	152	+925	<9	160	+159	<9	153	+931	<9	161	+160	<9	154	+937	<9	162	+161	<9	155	+943	<9	163	+162	<9	156	+949	<9	164	+163	<9	157	+955	<9	165	+164	<9	158	+961	<9	166	+165	<9	159	+967	<9	167	+166	<9	160	+973	<9	168	+167	<9	161	+979	<9	169	+168	<9	162	+985	<9	170	+169	<9	163	+991	<9	171	+170	<9	164	+997	<9	172	+171	<9	165	+1003	<9	173	+172	<9	166	+1009	<9	174	+173	<9	167	+1015	<9	175	+174	<9	168	+1021	<9	176	+175	<9	169	+1027	<9	177	+176	<9	170	+1033	<9	178	+177	<9	171	+1039	<9	179	+178	<9	172	+1045	<9	180	+179	<9	173	+1051	<9	181	+180	<9	174	+1057	<9	182	+181	<9	175	+1063	<9	183	+182	<9	176	+1069	<9	184	+183	<9	177	+1075	<9	185	+184	<9	178	+1081	<9	186	+185	<9	179	+1087	<9	187	+186	<9	180	+1093	<9	188	+187	<9	181	+1099	<9	189	+188	<9	182	+1105	<9	190	+189	<9	183	+1111	<9	191	+190	<9	184	+1117	<9	192	+191	<9	185	+1123	<9	193	+192	<9	186	+1129	<9	194	+193	<9	187	+1135	<9	195	+194	<9	188	+1141	<9	196	+195	<9	189	+1147	<9	197	+196	<9	190	+1153	<9	198	+197	<9	191	+1159	<9	199	+198	<9	192	+1165	<9	200	+199	<9	193	+1171	<9	201	+200	<9	194	+1177	<9	202	+201	<9	195	+1183	<9	203	+202	<9	196	+1189	<9	204	+203	<9	197	+1195	<9	205	+204	<9	198	+1201	<9	206	+205	<9	199	+1207	<9	207	+206	<9	200	+1213	<9	208	+207	<9	201	+1219	<9	209	+208	<9	202	+1225	<9	210	+209	<9	203	+1231	<9	211	+210	<9	204	+1237	<9	212	+211	<9	205	+1243	<9	213	+212	<9	206	+1249	<9	214	+213	<9	207	+1255	<9	215	+214	<9	208	+1261	<9	216	+215	<9	209	+1267	<9	217	+216	<9	210	+1273	<9	218	+217	<9	211	+1279	<9	219	+218	<9	212	+1285	<9	220	+219	<9	213	+1291	<9	221	+220	<9	214	+1297	<9	222	+221	<9	215	+1303	<9	223	+222	<9	216	+1309	<9	224	+223	<9	217	+1315	<9	225	+224	<9	218	+1321	<9	226	+225	<9	219	+1327	<9	227	+226	<9	220	+1333	<9	228	+227	<9	221	+1339	<9	229	+228	<9	222	+1345	<9	230	+229	<9	223	+1351	<9	231	+230	<9	224	+1357	<9	232	+231	<9	225	+1363	<9	233	+232	<9	226	+1369	<9	234	+233	<9	227	+1375	<9	235	+234	<9	228	+1381	<9	236	+235	<9	229	+1387	<9	237	+236	<9	230	+1393	<9	238	+237	<9	231	+1399	<9	239	+238	<9	232	+1405	<9	240	+239	<9	233	+1411	<9	241	+240	<9	234	+1417	<9	242	+241	<9	235	+1423	<9	243	+242	<9	236	+1429	<9	244	+243	<9	237	+1435	<9	245	+244	<9	238	+1441	<9	246	+245	<9	239	+1447	<9	247	+246

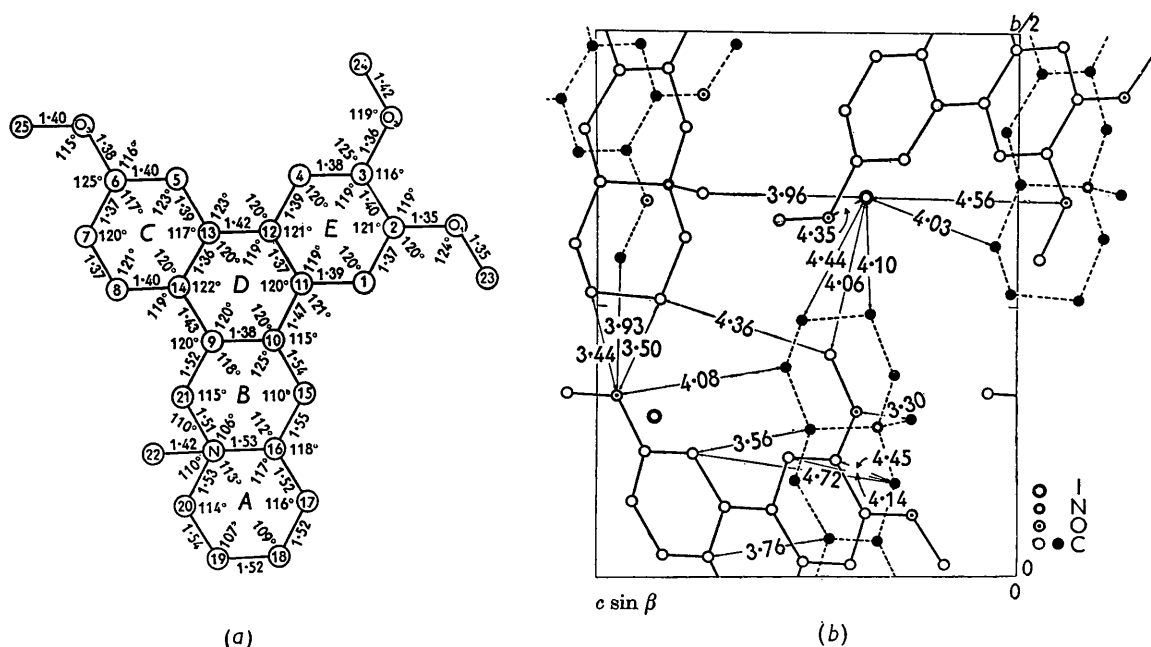
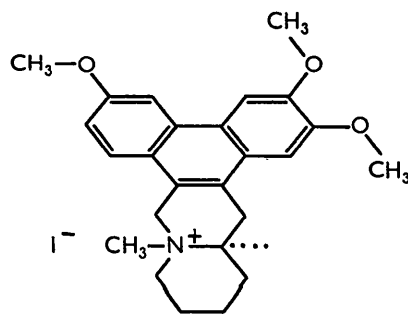


Fig. 6. (a) Intramolecular bond lengths and angles in DL-isocryptopleurine methiodide. (b) The packing arrangement of molecules in the crystal is indicated by a selection of the more important intermolecular approach distances. The area shown is $y = 0$ to $\frac{1}{2}b$, and $z = 0$ to $c \sin \beta$.

Table 5

Type of bond	No. of bonds	Mean value (Å)	Mean departure (Å)	Maximum departure (Å)	Standard value (Å)
C-C (aromatic)	16	1.39	0.02	0.08	1.39
C-C (aliphatic)	7	1.53	0.01	0.02	1.54
C-O	6	1.38	0.02	0.04	1.42
C-N	4	1.50	0.04	0.08	1.49

2':3':6'-trimethoxyphenanthro (9':10'-2:3) quinolizidine methiodide. (I)



(I)

This analysis appears to constitute the first observation of the phenanthro (9':10'-2:3) quinolizidine ring system. The natural product, L-cryptopleurine, may be merely the L form of 'DL-isocryptopleurine' or may differ from it in the configuration and/or the conformation of the quinolizidine moiety. Any difference be-

tween cryptopleurine and isocryptopleurine must lie in the AB ring system, particularly in relation to the nitrogen atom since the conversion of L-cryptopleurine to DL-isocryptopleurine occurs only through the methiodide (Gellert & Riggs, 1954). The presence of the quinolizidine ring system in isocryptopleurine (and perhaps in cryptopleurine) suggests that these compounds may be assigned to the lupinane group of alkaloids (Henry, 1949).

The locations of the atoms have been determined by the use of generalized projections, without ambiguity and more precisely than would be possible with normal projections (compare $|_3q_1|$ (Fig. 3(c)) and $|_2q_5|$ (Fig. 4(c)) with $_2q_0$ (Fig. 5(a))). The y, z coordinates derived from q_x (Fig. 5(b)) should be almost as accurate as if derived from a complete three-dimensional synthesis, but the x parameters are less precise. No attempt has been made to estimate series-termination errors. The iodine atom is probably located within 0.02 Å. For the light atoms, an estimate of accuracy can be made by considering the departure from the mean value for groups of bonds of the same type (Table 5). The mean and maximum departures are of a similar order to that noted in the refinement of

potassium benzylpenicillin (Pitt, 1952), which used 1680 hkl reflexions, whereas the analysis of *isocryptopleurine* methiodide used only 1070 selected reflexions. The bond-length determinations in the present study are therefore probably accurate to within 0.05 Å, adequate to define the molecule and to differentiate the types of bonds when the different species of atoms are distinguished and the configuration around each atom is taken into account.

The molecule is approximately planar, with only $C_{(22)}$ projecting from the general plane of the molecule. The packing of the molecules is mainly determined by their approximately planar shape and the required proximity of the iodine anions. The principal ion-molecule and molecule-molecule approach distances are listed in Table 3 and shown in Fig. 6(b). The closest approach of the iodine anion to nitrogen is indicated by $I-C_{(22)}$, 3.96 Å, while the remaining minimal ion-molecule approach distances are in the range 3.9–4.1 Å, in accordance with normal packing considerations. The approach distances between molecules are normal, the shortest being $C_{(22)}-O_{(2)}$, 3.30 Å. In general, the approach distances involving an oxygen atom are rather shorter than those involving two carbon atoms (CH_3 or CH_2).

The shape of the molecule and its orientation in the unit cell can be correlated with the wide variation in temperature factor, B (Table 1). The plane of the molecule is approximately parallel to $(2\bar{1}1)$ and, since the maximum thermal vibration of the atoms is perpendicular to the plane of the molecule, the hkl reflexions are affected to a greater extent than the $0kl$ reflexions. This is borne out by the particular values of B .

Generalized projections ($\rho_n = C_n + iS_n$), or rather the component projections, C_n and S_n , have been used mainly to study details of structure (Zachariasen, 1954) and to fix and refine the third (say z) parameters in analyses of 'heavy atom' derivatives of organic compounds (Dyer, 1951; Cochran & Dyer, 1952; Zussman, 1953). Although useful for such refinements, the component projections cannot generally be used to solve crystal structures unless the approximate molecular structure is known from chemical or physicochemical data and can be fitted to the normal projection so that correct points in component projections can be sampled (in particular, see Dyer, 1951; Zussman, 1953).

To solve crystal structures of this type (i.e. 'heavy atom' derivatives) with no assumptions regarding the shape of the molecule, the modulus projection, $|\rho_n| = [C_n^2 + S_n^2]^{\frac{1}{2}}$, offers many advantages. The possibility of deriving a modulus projection was first noted by Clews & Cochran (1949) but was used to provide accurate two-dimensional parameters. The principal advantage of the modulus projection appears to lie in the fact that the evidence regarding the third dimension contained in the component projections in terms of heights of peaks is obliterated and the available *three-dimensional data are compressed into two*

dimensions. From this arises its power in solving structures, since as many views of the projection can be obtained as there are layers. Because each layer represents completely independent experimental data, the errors in each modulus projection will be different. Hence, as shown in § 3, the various modulus projections can be combined so as to reduce spurious peaks and accentuate real ones. By this means, the correct molecular model *in projection* can be determined directly from the diffraction data. From then on, the normal use of component projections permits the determination and refinement of the third (z) parameters.

In addition to refining z parameters, modulus projections can assist in obtaining x , y parameters more accurate than those derived from the normal projection. This is particularly well illustrated by comparison of Fig. 3(c) and Fig. 5(a).^{*} The atomic parameters from individual modulus projections can be combined to yield a mean value or the modulus projections can be combined to form one projection, ρ_x , from which final parameters are measured. Clews & Cochran (1949) used the former method while we have favoured the latter (Fig. 5(b)) since it appears to give due weight to each layer. Apart from the undoubted improvement in accuracy due to combining several modulus projections, it is probable that the individual modulus projection (particularly corresponding to the lower layers) is more accurate than the normal zero-layer projection. Thus, in many cases, the first layer contains twice as many reflexions as the zero layer, owing to the particular space group and projection axis, e.g. in $P2_1/n$, $n(1kl) \approx 2n(0kl)$ and $n(h1l) \approx 2n(h0l)$. The positive and negative excursions of the functions C_n and S_n lead to an apparent improvement in resolution which may be by its nature partly spurious. However, where atoms overlap it is often possible to select a suitable layer for which one component of the corresponding generalized projection will give a clear view of the selected atom. The greater resolution of higher-layer projections over those of lower order has been ascribed by Phillips (1954) to the flatter range of the scattering curves for such layers, but often the amount of data has decreased appreciably, counterbalancing this effect (cf. Figs. 3(c) and 4(c)).

When two atoms of the same atomic number coincide in the normal projection (peak height, $2p$), either fortuitously or owing to the presence of a mirror plane, the height of the peak in the modulus projection ranges from $\frac{1}{2}p$, when atoms are separated by $\frac{1}{4}c$, to zero, when atoms are separated by $\frac{1}{2}c$ (where c is the projection axis). This effect may constitute the main dis-

^{*} The improved peak separation also played a part in aiding solution of the crystal structure, for it is dubious if this structure (in which one molecule overlaps the other) would have been soluble by normal projections alone (even if they could have been refined). It would have been difficult clearly to differentiate x , z parameters of atoms of approximately the same y parameter (Fig. 5(a) and (c)).

advantage of the modulus projection for solving complex structures, but there is a slight compensation in the reciprocal relationship: namely that if overlap leads to a small peak height in a modulus projection, the contributions of these two overlapping atoms to the structure amplitudes of that particular layer are correspondingly small. Also, it is somewhat rare for complete overlap to occur fortuitously, and when initiating a crystal analysis with modulus projections the projection axis with the greatest probability of clear projection should be chosen.

Finally, modulus projections have the advantage that 'heavy atom' derivatives of complex organic molecules can be solved *ab initio* with partial three-dimensional data, thus placing analysis within the scope of laboratories not equipped with automatic computers for handling the complete three-dimensional data otherwise necessary for these compounds.

References

- BEEVERS, C. A. (1952a). *Acta Cryst.* **5**, 670.
 BEEVERS, C. A. (1952b). *Acta Cryst.* **5**, 673.
 BUERGER, M. J. (1951). *Acta Cryst.* **4**, 531.
 CARLISLE, C. H. & KING, G. S. D. (1954). *Acta Cryst.* **7**, 627.
 CLEWS, C. J. B. & COCHRAN, W. (1949). *Acta Cryst.* **2**, 46.
 COCHRAN, W. & DYER, H. B. (1952). *Acta Cryst.* **5**, 634.
 DYER, H. B. (1951). *Acta Cryst.* **4**, 42.
 FRIDRICHSONS, J. & MATHIESON, A. McL. (1954a). *Nature, Lond.* **173**, 732.
 FRIDRICHSONS, J. & MATHIESON, A. McL. (1954b). *Acta Cryst.* **7**, 652.
 GELLERT, E. & RIGGS, N. V. (1954). *Austral. J. Chem.* **7**, 113.
 HASSEL, O. (1953). *Quart. Rev. Chem. Soc., Lond.* **7**, 221.
 HENRY, T. A. (1949). *The Plant Alkaloids*, p. 120. London: Churchill.
Internationale Tabellen zur Bestimmung von Kristallstrukturen (1935). Berlin: Borntraeger.
 JOEL, N., VERA, R. & GARAYCOHEA, I. (1953). *Acta Cryst.* **6**, 465.
 McWEENY, R. (1951). *Acta Cryst.* **4**, 513.
 MATHIESON, A. McL. (1955). *Rev. Pure Appl. Chem.* **5**, 113.
 PHILLIPS, D. C. (1954). *Acta Cryst.* **7**, 221.
 PITT, G. J. (1952). *Acta Cryst.* **5**, 770.
 ZACHARIASEN, W. H. (1954). *Acta Cryst.* **7**, 305.
 ZUSSMAN, J. (1953). *Acta Cryst.* **6**, 504.

Acta Cryst. (1955). **8**, 772

A New Method for Calculating the Effect of the Collimating System on the Small-Angle X-ray Scattering Pattern

BY PAUL W. SCHMIDT

Department of Physics, University of Missouri, Columbia, Mo., U.S.A.

(Received 11 April 1955 and in revised form 26 May 1955)

The angular distribution of small-angle X-ray scattering, corrected for the effects of the collimating system, is expressed in terms of the pair distribution function. This formulation, which has not previously been used for determination of collimation corrections, is convenient when the slit height or scattering angle is large. When the slits are of infinite height and negligible width, the slit-corrected functions are almost as easy to calculate as the perfect-collimation functions. Evaluation in terms of known functions is made for hollow spheres of uniform charge density, and the results are tabulated. The use of the tables for analysis of scattering data is described.

1. Introduction

In recent years the scattering of X-rays at angles of 5° or less has been used to gain information about the size and shape of particles in the size range 20–2000 Å, including several viruses and proteins (Ritland, Kaesberg & Beeman, 1950; Leonard, Anderegg, Shulman, Kaesberg & Beeman, 1953; Schmidt, Kaesberg & Beeman, 1954). Under these conditions the small-angle scattering is due to diffraction from small particles and is little affected by atomic structure.

A common practice in the analysis of the scattering data is to compare the experimental scattering curves

with scattering curves calculated under the assumption of a dilute solution of identical particles of a particular shape. This procedure is in practice usually preferable to an inversion of the scattering curve, because there may be sufficient uncertainty in the data to make the inverted curve unreliable and because of the difficulty of relating the inverted curve unambiguously to the particle size and shape.

Theoretical scattering patterns have been calculated for a few simple shapes, assuming perfect collimation (Fournet & Guinier, 1950; Porod, 1948–9). However, with collimating slits of the size usually needed to obtain sufficient scattered intensity, the effects of the